Manipulated Electrospun PVA Nanofibers with Inexpensive Salts

Wei Ding, Suying Wei,* Jiahua Zhu, Xuelong Chen, Dan Rutman, Zhanhu Guo*

PVA nanofibers have been successfully prepared via an electrospinning process by optimizing the electrospinning operational parameters including applied voltage, polymer concentration, feed rate, and working distance. Inexpensive NaCl and $Fe(NO_3)_3$ are found to reduce the fiber size drastically (minimum of 157 and 169 nm, respectively) even at a low loading. The thermal stability is investigated by both thermogravimetric analysis and differential scanning calorimetry. Fourier transform infrared spectroscopy is utilized to characterize the functionality of the fibers and to investigate the interaction between PVA and inorganic additions. Glass transition and melting temperatures of the PVA fibers have slight change with the increase of the salt loading.

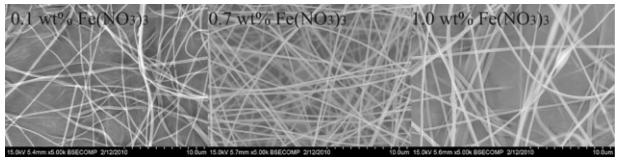

Introduction

Polymer fibers especially in the nanoscale have drawn tremendous interest for decades due to their unique physicochemical properties, such as large specific surface area, multiple surface functionalities and superior mechanical properties, which make them widely applied in various areas, such as membrane fabrications, tissue engineering, biomedical devices, and optical sensors.[1–4] Among the methods to fabricate fibers such as double crucible method, vapor phase oxidation, and plasma chemical vapor deposition, the relatively high voltage electrospinning is a highly valued technique for preparing fibers in nanoscale due to its low-cost set-up, simple operation, high-yield, and morphology-controllable characteristics.[1,5–10] The electrospinning process can be briefly described as follows. The polymer solution was loaded in a syringe. Once an electrical field generated between the syringe tip and the collecting electrode, polymer solution would be ejected by a pump. Under the applied electrostatic field strength, solvent in the ejected polymer solution evaporated during flight and the polymer was stretched due to the charge effect of solution, and thus formed nanofibers in different morphologies.[11] An aluminum foil that covered the electrode was used to collect the formed fibers. The experiment operational conditions are reported to have significant influence on the final fibers.[12–17]

Poly(vinyl alcohol) (PVA) is a water-soluble and biodegradable polyhydroxy polymer that has been studied intensively due to its good thermal stability, biocompatibility, chemical resistance, and inexpensiveness.[18–21] In particular, its aqueous solution is transparent, colorless, and nontoxic. Hong et al. reported PVA nanocomposites fibers reinforced with Ag nanoparticles as wound dressing.[22] Sajeev et al. mentioned that nanoscale PVA fibers had been applied as reinforcing fillers, filtration materials, tissue scaffoldings, releasing vehicles of drugs, and so forth.[16] Nanocomposite fiber fabrication based on PVA via electrospinning was reported abundantly.[16,18–25] Some references reported the influence of inorganic addition on the properties of nanoscale fibers.[17,26] However, there are few reports regarding the salt effect on the morphology of the fibers, especially sodium chloride and iron(III) nitrate, these two commonly used electrolytes.

In this paper, the optimum condition to prepare pure PVA fibers has been explored. The operational parameters such as volume federate, applied voltage, polymer concentration, and the tip-to-electrode distance have been systematically investigated. Sodium chloride and iron nitrate are

W. Ding, S. Y. Wei, J. H. Zhu, X. L. Chen, D. Rutman, Z. H. Guo
Integrated Composites Laboratory, Lamar University, Beaumont, TX 77710, USA
E-mail: zhanhu.guo@lamar.edu; suying.wei@lamar.edu

DOI: 10.1002/mame.201000188

observed to have a significant effect on the fiber morphology even at a pretty low content.

Experimental Part

Materials

PVA (molecular weight = 88 000–96 800, degree of polymerization = 2 000–2 200) was provided by Sigma-Aldrich Company. Sodium chloride (NaCl, Granular/USP/FCC) is purchased from Fisher Scientific Company. Iron(III) nitrate nonahydrate, [$Fe(NO_3)_3 \cdot 9H_2O$, ACS, 98.0–101.0%] was obtained from Alfa Aesar. All the chemicals were used as received without any further treatment. De-ionized water was used as solvent.

Polymer Solution Preparation

PVA was dissolved in de-ionized water at 80 °C with vigorous magnetic stirring. The polymer concentrations were 9.0, 10.0, and 11.0 wt.-%, respectively.

NaCl with a concentration of 0.1, 0.2, 0.3, 0.5 and 1.0 wt.-% (with respect to the weight sum of PVA and NaCl) was added into the pure PVA solution, respectively. Similarly, $Fe(NO_3)_3$ with a concentration of 0.1, 0.3, 0.5, 0.7, and 1.0 wt.-% was dissolved in PVA aqueous solution.

Fiber Fabrication from Pure PVA and PVA/Salts

PVA/NaCl, PVA/$Fe(NO_3)_3$, and pristine PVA solutions were used during the electrospinning process. Operational parameters such as applied voltage (10, 15, and 20 kV), feed rate (8, 10, and 10 $\mu L \cdot min^{-1}$) and tip-to-collector distance (8, 10, 12, and 16 cm) were adjusted to obtain the optimum nanofibers.

Electrospinning Setup

A typical electrospinning setup was used in this study. A 5 mL syringe with a stainless-steel needle (inner diameter 0.6 mm) was used to transfer polymer solution to the needle tip. A high-voltage power supply (Gamma High Voltage Research, Product HV power Supply, Model No. ES3UP-5w/DAM) was utilized to control the applied electrical voltage, which was in the range 0 to 30 kV. The polymer solution loaded in the syringe was ejected by a syringe pump (NE-300, New Era Pump Systems, Inc.) with an accurate and controllable feed rate. The fabricated nanoscale fibers were then collected on an aluminum foil, which was connected to the ground and acted as the fiber collector.

Characterizations

Scanning electron microscopy (SEM, Hitachi S-3400) was used to characterize the microstructure of pure PVA, PVA/NaCl and PVA/$Fe(NO_3)_3$ fibers. The morphology (length and diameter) of the fibers was measured by software Quartz PCI version 7.

The rheological behavior of the aqueous polymer solution was examined by a Rheometer (AR 2000ex, TA Instrumental Company). The operation shear rate was varied from 1.0 to 1 000 rad $\cdot s^{-1}$ at 25 °C. A series of measurements were performed in a cone-and-plate geometry with a diameter of 40 mm and a truncation of 66 μm.

Thermogravimetric analysis (TGA, Q-500) and differential scanning calorimetry (DSC) were applied to investigate the thermal stability of the fibers. The thermal decomposition of the PVA fibers was determined by means of TGA from 25 to 1000 °C with an air flow rate of 50 $cm^3 \cdot min^{-1}$ (ccpm) and a heating rate of 20 °C $\cdot min^{-1}$. The DSC temperature and heat flow values were calibrated. The heating and cooling rates were set at 10 °C $\cdot min^{-1}$ with a continuous nitrogen flow of 20 $cm^3 \cdot min^{-1}$. The temperature was in the range 25–250 °C.

The interaction and surface functionality between the salts and polymer matrix were characterized by Fourier-transform infrared (FT-IR, a Bruker Inc. Tensor 27 FT-IR spectrometer with hyperion 1000 ATR microscopy accessory) spectroscopy.

Results and Discussion

Microstructures of Pure PVA Fibers

Effect of PVA Concentration

Polymer concentration is an important operational parameter in the electrospinning process, which influences the fiber morphology significantly. The formation of the fibers is inhibited in the solutions with high concentrations due to their high viscosity.[17] The high viscosity makes the solutions extremely difficult to flow through the syringe needle to form nanofibers under an electrostatic force.[15] Therefore, appropriate solution concentration becomes one of the key parameters to optimize the final electrospinning fibers.

Figure 1 shows the SEM images of the electrospun pure PVA fibers from solutions with a concentration of 9.0, 10.0, and 11.0 wt.-%, respectively. Under the same experimental condition, the average diameter of the PVA nanofibers becomes larger with the increase of the solution concentration. The average fiber diameter is 139, 165, and 189 nm for the solutions with a concentration of 9.0, 10.0, and 11.0 wt.-%, respectively. However, the fibers are nonuniform when the solution concentration is relative low, Figure 1(a). Some beads are also observed due to the lack of force balance among the electrostatic repulsion, surface tension, and viscoelastic force.[27,28] The surface tension of the solution and the electrostatic force should be balanced to obtain the stable jets in order to form continuous fibers. Once the applied voltage exceeds the critical voltage, the jets of the liquids will get ejected from the cone tip. The jets will not be stable, which is responsible for the bead formation (sometimes is called electrospray if the beads are separate particles) if the solution viscosity is extremely low. In the solution with relatively high viscosity, the stable jets without breaking due to the cohesive nature of the high viscosity, travel to the electrode and finally form the

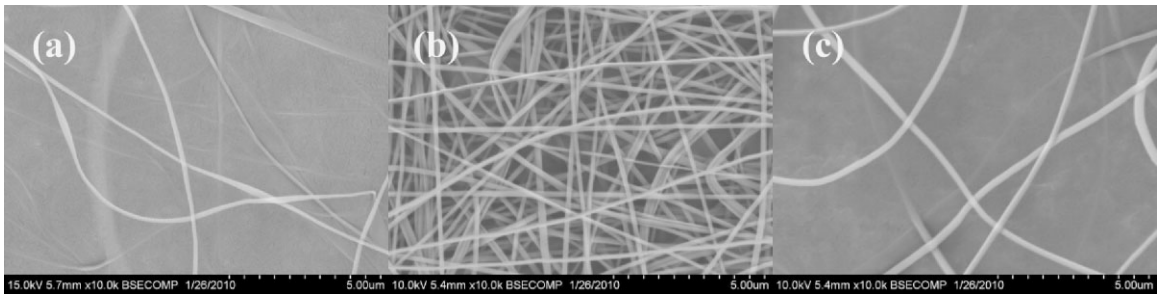

Figure 1. SEM microstructures of pure PVA nanofibers fabricated at a concentration of (a) 9.0, (b) 10.0, and (c) 11.0 wt.-%. Applied voltage 20 kV, feed rate 10 $\mu L \cdot min^{-1}$, working distance 10 cm.

uniform fibers on the collecting grounded electrode, Figure 1(b, c).

Effect of Applied Voltage

The applied electrical voltage has an evident influence on the fiber's morphology. Figure 2 shows the SEM microstructure of the PVA fibers fabricated from 11.0 wt.-% PVA solution under different applied electrical voltages. The fiber diameters are observed to decrease with the increase of the applied electrical voltage. The electric field strength is known to increase with the increase of the applied voltage. However, a critical voltage is required in order to obtain the cone for fiber formation even though the working distance is very small with very strong electric field strength. The increase in the electric field strength should result in an enhancement in the electrostatic force on the solution jet, which will facilitate the thinner fiber formation.[16] The average fiber diameters decrease from 296 to 161 nm with the increase of the applied voltage. At a lower applied voltage (10 kV), some secondary spun fibers with different sizes are observed, which are about two fifth as compared to the size of the primary ones. This observation is in consistence with the results obtained in poly(ethylene oxide) (PEO)/water solution, which shows obvious more secondary population of the fibers with diameters about one-third of those in the primary population.[29] This observed bimodal fiber distribution is due to the fiber splaying events, which has been reported by Doshi and Reneker[30] in spinning the PEO fibers from a relatively higher concentration. However, at a higher applied electrical voltage (20 kV), fibers with more uniform sizes are observed, Figure 2(c). High voltage is able to generate more charges to the solution or droplet surface located at the tip of the needle (larger Coulombic forces) as well as a stronger electrical field (larger electrostatic forces), both of which will stretch the jets fully for the favorable formation of the uniform and smooth fibers.[17,31]

Effect of Feed Rate

It has been pointed out that the feed rate of the polymer solution influences strongly on the polymer fiber morphology.[29] However, this is not always the case. Figure 3 shows the SEM microstructures of the PVA fibers fabricated from 10.0 wt.-% PVA solutions at a constant working distance of 10 cm, a fixed applied electrical voltage of 20 kV, and different flow rates. With increasing feed rate, the average diameter is observed to increase from 174 to 179 nm. This indicates that the morphology, diameter size, and uniformity of the electrospun PVA fibers are not significant influenced by the feed rate. Once the federate is sufficient enough to form fibers, a higher federate will supply more PVA solution and is recognized as excess, which will produce fibers with beads.[17] Here, uniform fibers are still observed even at a flow rate of 12 $\mu L \cdot min^{-1}$, which favors fiber production with a larger yield.

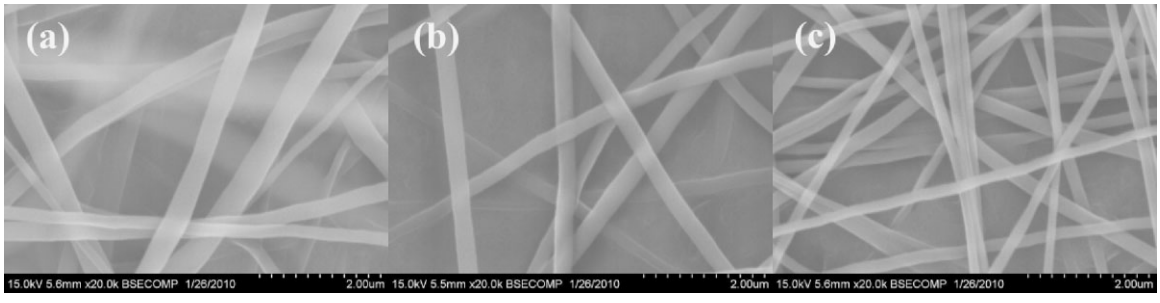

Figure 2. SEM images of 11.0 wt.-% pure PVA nanofiber under different applied voltages. Feed rate 10 $\mu L \cdot min^{-1}$, working distance 10 cm. Applied voltage (a) 10, (b) 15, (c) 20 kV.

Macromol. Mater. Eng. **2010**, *295*, 958–965

Macromolecular Journals
DOI: 10.1002/mame.201000188

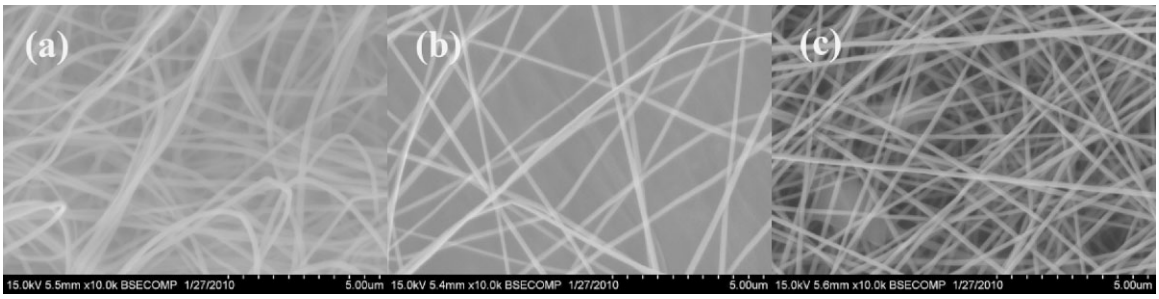

Figure 3. Feed rate effect: SEM images of 10 wt.-% pure PVA nanofibers. Applied voltage 20 kV, working distance 10 cm. Feed rate (a) 8, (b) 10, (c) 12 $\mu L \cdot min^{-1}$.

Effect of Tip-to-Collector Working Distance

Polymer jets are stretched under electrostatic force when they travel through the electrical field. During this process, solvent evaporates and the polymer jets maintain their elasticity. It is reported that the chance of the fiber contraction (shrinkage) increases with the increase of the working distance.[15]

To evaluate the effect of working distance between the needle tip to collector on the morphology of the electrospun PVA nanofibers, the experiment is carried out with a constant concentration of 10.0 wt.-% PVA solution under 15 kV. The working distances are controlled at 8, 10, 12, and 16 cm, respectively. Figure 4 shows the observed SEM microstructures of the pure PVA fibers fabricated from the above operational conditions. The working distance is observed to have significant effect on the morphology of the PVA nanofibers. However, the experimental phenomena have some deviation from the previous observations.[32] With the working distance increases from 8 to 10 cm, the beads that act as defects disappear, and the fibers become thinner (from 266 to 93 nm). The fiber diameter is observed to decrease and uniformity is to increase gradually with the increase of the working distance. The observed beads and non-uniform fibers, Figure 4(a,b) are due to the unstable jet flow arising from the unbalanced forces among the above mentioned three forces with a short working distance induced larger electrostatic force.[33] The secondary spun fibers still exist until the working distance reaches 12 cm. At this working distance, nanofibers are formed uniformly (109 to 149 nm). When the working distance increases to 16 cm, the uniformity of the fibers decreases and even some cracks are observed in the PVA fibers. This is due to the fibers with an electrostatic force not strong enough to resist the breakage from the electric field induced stretch.

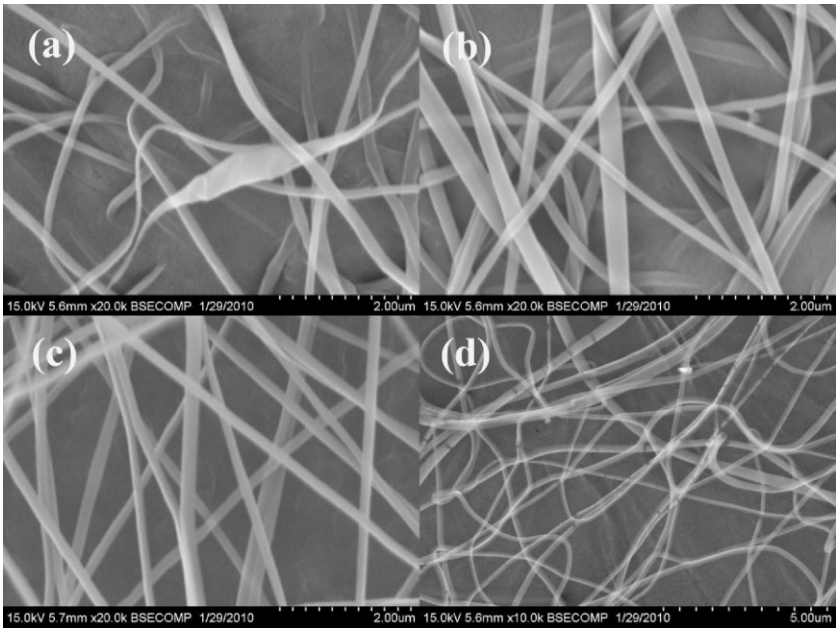

Figure 4. Working distance effect: SEM images of 10 wt.-% pure PVA nanofibers. Feed rate 10 $\mu L \cdot min^{-1}$, applied voltage 15 kV. Working distance (a) 8, (b) 10, (c) 12, (d) 16 cm.

The Effect of NaCl on the Morphology of PVA Fibers

The introduction of salts increases the surface charge density and the electrical conductivity of the solution.[17] The force balance among the surface tension, viscoelastic, and electrostatic forces for the polymer solution will be changed and will influence the morphology of electrospun nanofibers. The addition of ionic salt to the polymer solution is observed to reduce the bead formation and to decrease the fiber diameter.[34] However, the effects of the salt concentration and the optimum salt concentration on the formed fibers have not been studied.

At the operational condition of 15 kV and 9 cm, fibers electrospun from 11.0 wt.-% pristine PVA solution are non-uniform and possess some beaded defects. However, the beads disappear in the electrospun fibers though the fibers

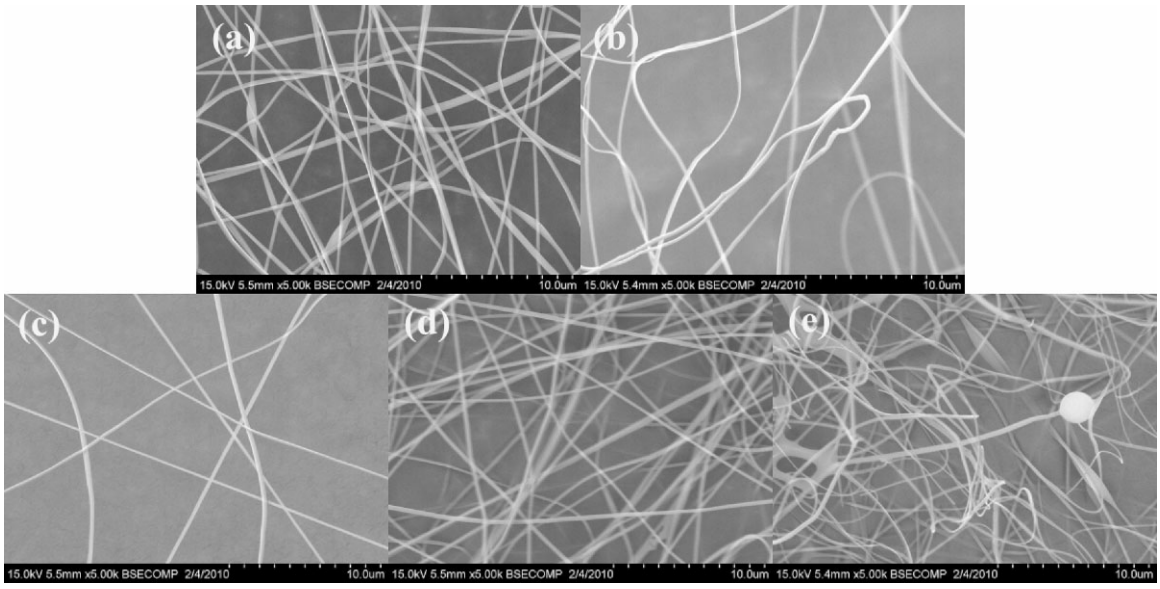

Figure 5. SEM images of 11 wt.-% PVA nanofibers with NaCl concentrations of (a) 0.1, (b) 0.2, (c) 0.3, (d) 0.5, (e) 1.0 wt.-%. Applied voltage 15 kV, working distance 9 cm, feed rate 8 $\mu L \cdot min^{-1}$.

are nonuniform after the addition of 0.1 wt.-% NaCl (with respect to the weight sum of NaCl and PVA) in the pristine PVA solution. When NaCl content increases to 0.3 wt.-%, the fibers decrease in size and have a very narrow size distribution. However, as the NaCl concentration increases further, secondary spun fibers and beads appear again [Figure 5(d,e)]. Thus, an appropriate amount of NaCl facilitates the formation of uniform PVA fibers. PVA solution with a higher loading of NaCl results in a decreased uniformity of the fibers and generates beaded defects. This is due to the excessive amount of NaCl dissolved in the PVA solution, which increases the ionic strength and makes the ejected polymer force unbalanced among the surface tension, viscoelastic, and electrostatic forces.

The Effect of Iron (III) Nitrate on the Morphology of PVA Fibers

Similar experiments are conducted on $Fe(NO_3)_3$. Figure 6 shows the SEM images of the fibers from the polymer

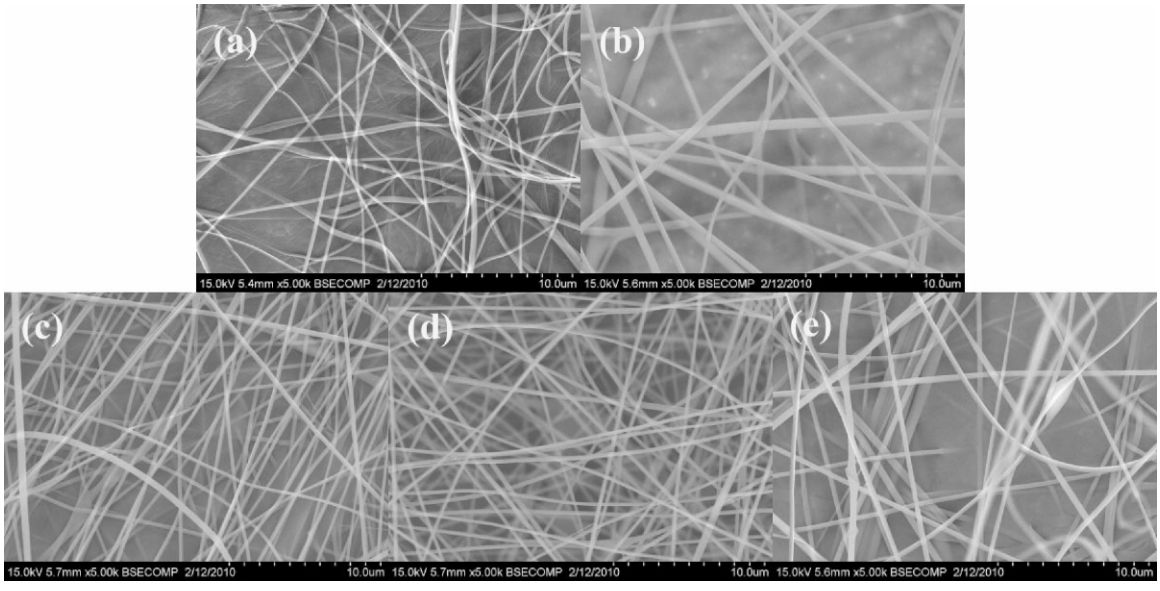

Figure 6. SEM images of 11 wt.-% PVA nanofibers with different $Fe(NO_3)_3$ concentrations: (a) 0.1, (b) 0.3, (c) 0.5, (d) 0.7, (e) 1.0 wt.-%. Applied voltage 15 kV, working distance 9 cm, feed rate 8 $\mu L \cdot min^{-1}$.

Macromol. Mater. Eng. **2010**, *295*, 958–965

Macromolecular Journals
DOI: 10.1002/mame.201000188

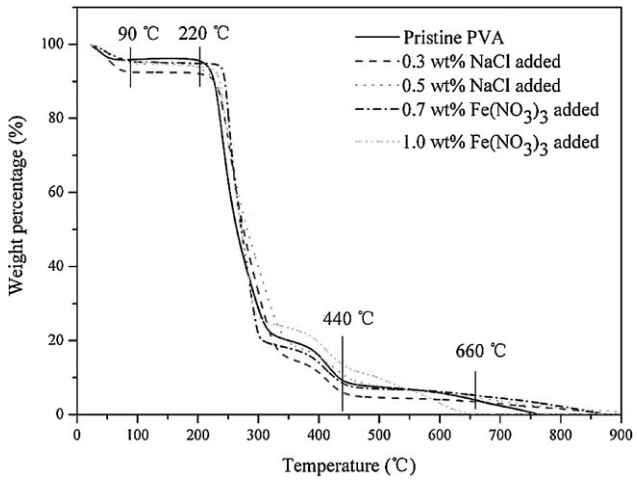

Figure 7. TGA curves of PVA/NaCl and PVA/$Fe(NO_3)_3$ nanocomposite fibers.

solution with the addition of iron nitrate. The uniformity of the nanofibers increases and the diameter decreases gradually with the concentration of $Fe(NO_3)_3$ increasing from 0.1 to 0.5 wt.-%. Once the content of $Fe(NO_3)_3$ reaches 0.7 wt.-%, the nanofibers are within 127 ± 43 nm. However, when the content of $Fe(NO_3)_3$ reaches 1.0 wt.-%, non-uniform fibers and beads appear again, which are consistent with the above observation in the NaCl case. The diameters of the fibers at different salt contents are compared and shown in Figure 8. Compared with the pristine PVA fibers, fibers with both narrowly distributed diameter and more uniformity are obtained while 0.3 wt.-% NaCl and 0.7 wt.-% $Fe(NO_3)_3$ are mixed with PVA solution, respectively. This demonstrates that an appropriate amount of salt can decrease the fiber diameter and enhance the fiber's quality effectively. Figure 8 summarizes the fiber diameters fabricated from PVA solution (11.0 wt.-%) with different salt concentrations.

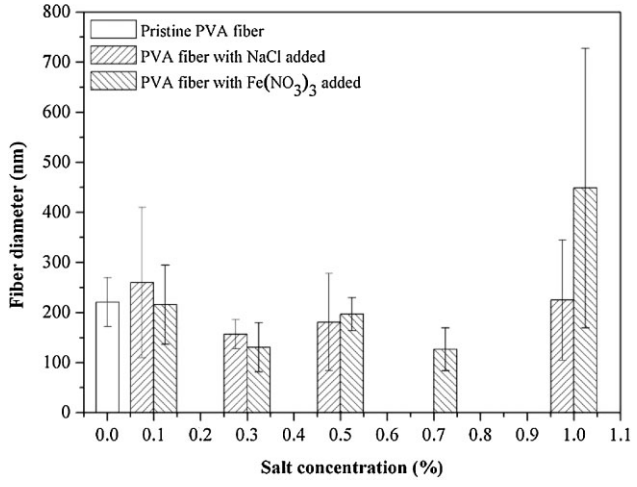

Figure 8. Different salt concentrations in 11.0 wt.-% PVA solution and the final average nanofiber diameters. Applied voltage 15 kV, working distance 9 cm, feed rate 8 $\mu L \cdot min^{-1}$.

Thermal Analysis

TGA

Figure 7 shows the thermogravimetric analysis curves of the pristine PVA fibers, PVA/NaCl and PVA/$Fe(NO_3)_3$ fibers with different salt loadings. Three main weight loss stages are observed. A small weight percentage loss is observed at lower temperature below 90 °C, which corresponds to the evaporation of the adsorbed moisture. The second weight loss stage is between 220 and 440 °C, which is predominated by the decomposition of the side chains of PVA. The major weight loss is observed in the second stage and then followed by a further smaller weight loss in the third stage in the range of 440 to 660 °C, which is attributed to the decomposition of the main chain of PVA.[21] It is noticed that more than 80 wt.-% PVA fibers are decomposed within the second and third stages. According to the thermograms, the small amount of salt does not influence the thermal degradation of PVA and PVA based nanocomposite fibers significantly. However, with the increase of the $Fe(NO_3)_3$ loading to 1.0 wt.-%, the decomposition rate increases dramatically as compared to that of the other PVA based nanofibers. That is due to the fact that $Fe(NO_3)_3$ enhances the degradation rate of PVA by serving as the known oxidizing agent (oxidant). In the other words, low percentage of salt addition does not modify the physical structure of PVA, and thus maintains the thermal stability, which is similar to that of the pristine PVA fibers.

DSC

PVA is a semi-crystalline polymer exhibiting both glass transition temperature (T_g) and melting temperature (T_m). Due to the introduction of the salts, the thermal behavior of PVA based nanocomposite fibers is expected to be affected in terms of the interaction between chemical compositions.[35] Figure 9 shows the DSC curves of the pristine PVA and PVA/NaCl nanocomposite fibers with a NaCl loading of 0.1 and 0.5 wt.-%, respectively. Glass transition temperature at 82 °C is observed for the pristine electrospun PVA nanofibers. With the increase of the NaCl loading, the glass transition temperature increases from 89 to 95 °C, which is due to the introduced interaction between the PVA and the salt ions as justified by the following FT-IR analysis.

The second endothermic peaks for the pristine PVA and PVA/NaCl nanocomposite fibers appearing at around 230 °C represent the melting of the crystalline PVA phase. Due to the low loaded salt, the melting temperatures are 230, 229, and 228 °C for pristine PVA, and PVA/NaCl fibers with a NaCl loading of 0.1 and 0.5 wt.-%, respectively. The

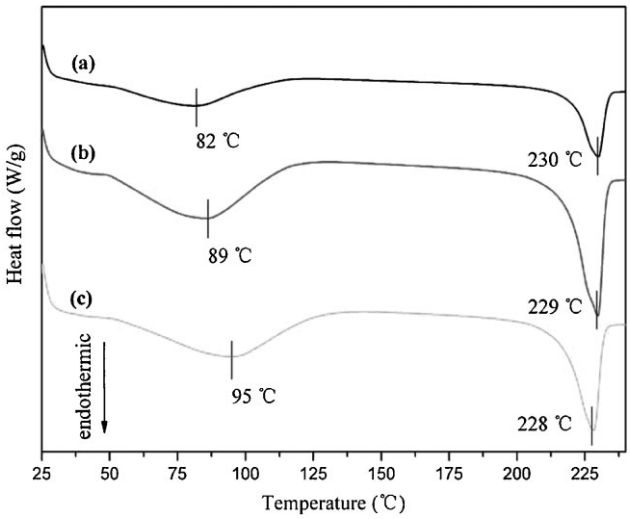

Figure 9. DSC curves of (a) pristine PVA, (b) PVA/NaCl with 0.3 wt.-%, and (c) 0.5 wt.-% nanocomposite fibers.

slightly lower glass temperature is due to the interaction between the ions and the polymer chains.

FT-IR Spectra

Figure 10 shows the FT-IR spectra of the pristine PVA and PVA-based nanocomposite fibers with different salt loadings. The peaks at 831, 1 088, 1 319, 1 413, 2 904, 2 949, and 3 288 cm^{-1} are the characteristic PVA absorption bands.[36,37] However, there are no specific absorption peaks except the ones appeared at 1 413 and 1319 cm^{-1}, which are corresponding to the C—C and $-CH_2$ stretch bands, respectively.[24] For the spectra, Figure 11(b) and (c) of 0.3 and 0.5 wt.-% NaCl, the ratios of relative height of

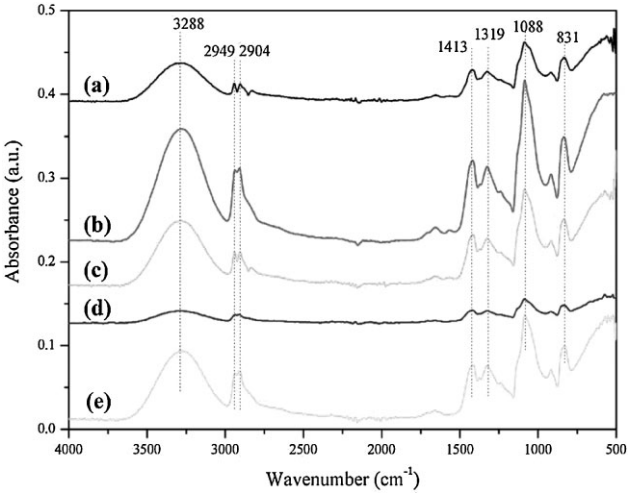

Figure 10. FT-IR spectra of (a) pristine PVA, (b) PVA/NaCl with 0.3 wt.-%, (c) 0.5 wt.-% loading, (d) PVA/$Fe(NO_3)_3$ with 0.7 wt.-% and (e) 1.0 wt.-% loading nanocomposite fibers.

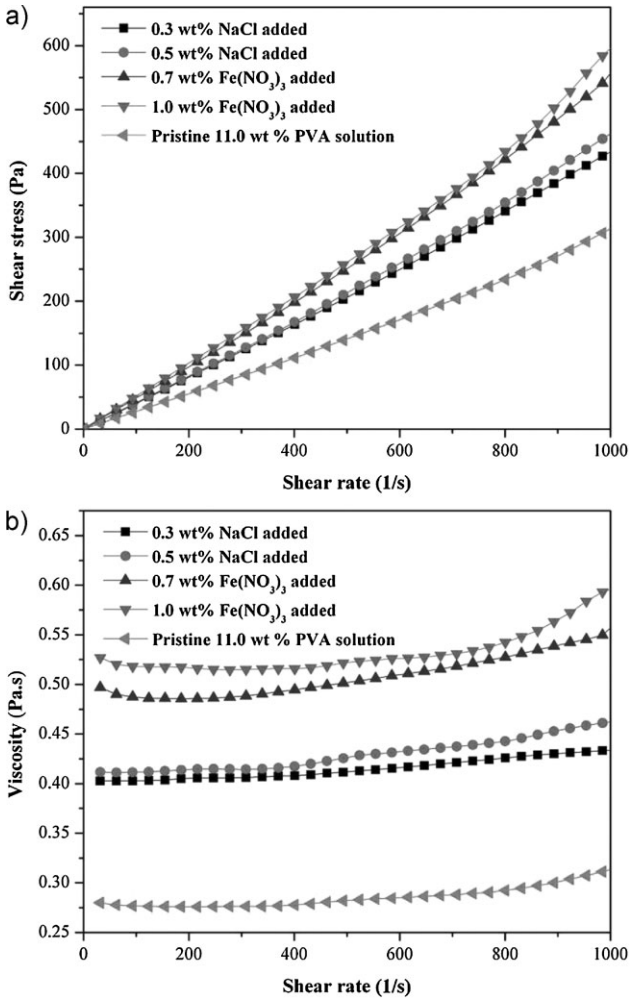

Figure 11. Rheological behavior analysis for (a) shear stress and (b) viscosity vs. shear rate of pristine PVA, PVA/NaCl, and PVA/$Fe(NO_3)_3$ solution with different salt loadings.

these two peaks are almost the same as compared to that of the pristine PVA. However, the peak intensity ratios of C—C and $-CH_2$ function groups is changed for the PVA fibers with 0.7 and 1.0 wt.-% $Fe(NO_3)_3$ as compared to the pure PVA fibers. This indicates that there is a strong interaction between the PVA matrix and the introduced salts. This is reasonable due to the polar structure of the polymer structure and the cations and anions of the salts, which are believed to have a strong interaction and is responsible for the observed thermal difference.

Rheological Behavior

Figure 11 shows the shear stress and viscosity as a function of shear rate for the PVA solutions with and without salts. The viscosity is observed to increase with the addition of salts. In addition, the viscosity increases further with the increase of the salt loading, Figure 10(b). The slight amount

Macromol. Mater. Eng. **2010**, *295*, 958–965

Macromolecular Journals
DOI: 10.1002/mame.201000188

of salt influences the ion intensity in PVA solution. The hydroxyl groups are the main function groups in PVA and they have tendency to form links with the salt ion. Therefore, the PVA chains align with each other and limit the mobility of PVA,[38] which is responsible for the observed higher viscosity in the NaCl/PVA solutions.

A linear relationship between the shear stress and the shear rate, Figure 10(a), is observed for almost all the solutions, which indicates a Newtonian flow.[39] The constant proportionality is expressed as the viscosity. Slightly loaded salt does not influence the linear relationship significantly and the viscosity is within the same magnitude. Therefore, the formed uniform fibers are influenced more by the ionic strength than by the viscosity.

Conclusion

Optimum condition to obtain the bead-free and uniform PVA nanofibers via electrospinning has been systematically investigated. Inexpensive sodium chloride and iron (III) nitrate are applied in pristine PVA aqueous solution and found to have a significant effect on the quality of nanofibers. An appropriate amount of salt facilitates the formation of slim and uniform nanofibers and eliminates the bead defects effectively. However, polymer solutions with more salts, such as 1.0 wt.-% $Fe(NO_3)_3$, provide non-uniform and beaded fibers. Thermal analysis is conducted by TGA/DSC. FT-IR spectrum analysis demonstrates that $Fe(NO_3)_3$ in the PVA fiber changes the ratio of C−C and $-CH_2$ function groups in PVA matrix and indicates a strong interaction between the PVA and the salt ions. The solution viscosities of the pristine PVA, PVA/NaCl, and PVA/$Fe(NO_3)_3$ increase slightly with the addition of small amount of salts. The ionic strength rather than the viscosity is responsible for the difference in the electrospun nanofibers.

Acknowledgements: This project was supported by the *Research Startup Fund* and a *Research Enhancement Grant* from *Lamar University*. W. Ding appreciates the research assistantship support from *Lamar University*.

Received: May 4, 2010; Published online: September 22, 2010; DOI: 10.1002/mame.201000188

Keywords: electrospun nanofibers; nanocomposites; rheology; salts

[1] Z.-M. Huang, Y. Z. Zhang, M. Kotaki, S. Ramakrishna, *Compos. Sci. Technol.* **2003**, *63*, 2223.
[2] T. G. Fox, J. B. Kinsinger, H. F. Mason, E. M. Schuele, *Polymer* **1962**, *3*, 71.
[3] E.-R. Kenawy, J. M. Layman, J. R. Watkins, G. L. Bowlin, J. A. Matthews, D. G. Simpson, G. E. Wnek, *Biomaterials* **2003**, *24*, 907.
[4] B. Ding, M. Yamazaki, S. Shiratori, *Sens. Actuators B* **2005**, *106*, 477.
[5] I. S. Chronakis, *J. Mater. Process. Technol.* **2005**, *167*, 283.
[6] A. T. Johnson Jr., N. J. Pinto, A. G. MacDiarmid, C. H. Mueller, N. Theofylaktos, D. C. Robinson, F. A. Miranda, *Appl. Phys. Lett.* **2003**, *83*, 4244.
[7] D. Li, Y. Wang, Y. Xia, *Nano Lett.* **2003**, *3*, 1167.
[8] W. E. Teo, S. Ramakrishna, *Int. J. Nanotechnol.* **2006**, 17.
[9] D. Zhang, A. B. Karki, D. Rutman, D. P. Young, A. Wang, D. Cocke, T. H. Ho, Z. Guo, *Polymer* **2009**, *50*, 4189.
[10] J. Zhu, S. Wei, X. Chen, A. B. Karki, D. Rutman, D. P. Young, Z. Guo, *J. Phys. Chem. C* **2010**, *114*, 8844.
[11] G.-M. Kim, G. H. Michler, P. Pötschke, *Polymer* **2005**, *46*, 7346.
[12] A. V. Melechko, M. A. Guillorn, D. H. Lowndes, M. L. Simpson, *Appl. Phys. Lett.* **2002**, *80*, 4816.
[13] C. Subramanian, R. A. Weiss, M. T. Shaw, *Polymer.* **2010**, *51*, 1983.
[14] M. M. Demir, I. Yilgor, E. Yilgor, B. Erman, *Polymer* **2002**, *43*, 3303.
[15] B. Ding, H.-Y. Kim, S.-C. Lee, D.-R. Lee, K.-J. Choi, *Fibers Polym.* **2002**, *3*, 73.
[16] U. Sajeev, K. Anoop Anand, D. Menon, S. Nair, *Bull. Mater. Sci.* **2008**, *31*, 343.
[17] V. Beachley, X. Wen, *Braz. J. Mater. Sci. Eng. C* **2009**, *29*, 663.
[18] S. C. Pitt Supaphol, *J. Appl. Polym. Sci.* **2007**, *108*, 969.
[19] A. S. Asran, S. Henning, G. H. Michler, *Polymer* **2010**, *51*, 868.
[20] Z. Guo, D. Zhang, S. Wei, Z. Wang, A. Karki, Y. Li, P. Bernazzani, D. Young, J. Gomes, D. Cocke, T. Ho, *J. Nanopart. Res.* **2010**, *12*, 2415.
[21] G.-M. Kim, A. S. Asran, G. H. Michler, P. Simon, J. S. Kim, *Bioinspir. Biomim.* **2008**, *3*, 046003.
[22] K. H. Hong, *Polym. Eng. Sci.* **2007**, *47*, 43.
[23] C. Shao, H.-Y. Kim, J. Gong, B. Ding, D.-R. Lee, S.-J. Park, *Mater. Lett.* **2003**, *57*, 1579.
[24] B. Suo, X. Su, J. Wu, D. Chen, A. Wang, Z. Guo, *Mater. Chem. Phys.* **2009**, *119*, 237.
[25] Z. H. Mbhele, M. G. Salemane, C. G. C. E. van Sittert, J. M. Nedeljkovic, V. Djokovic, A. S. Luyt, *Chem. Mater.* **2003**, *15*, 5019.
[26] Y.-Z. Chen, Z.-P. Zhang, J. Yu, Z.-X. Guo, *J. Polym. Sci., Part B: Polym. Phys.* **2009**, *47*, 1211.
[27] H. Fong, I. Chun, D. H. Reneker, *Polymer* **1999**, *40*, 4585.
[28] A. L. Huebner, *Science* **1970**, *168*, 118.
[29] J. M. Deitzel, J. Kleinmeyer, D. Harris, N. C. Beck Tan, *Polymer* **2001**, *42*, 261.
[30] J. Doshi, D. H. Reneker, *J. Electrostat.* **1995**, *35*, 151.
[31] D. Li, Y. Xia, *Adv. Mater.* **2004**, *16*, 1151.
[32] S. Sukigara, M. Gandhi, J. Ayutsede, M. Micklus, F. Ko, *Polymer* **2007**, *44*, 5721.
[33] Y. Y. Qiang Li, Z. Jia, L. Wang, Z. Guan, *International Conference on Solid Dielectrics* Winchester, UK July 8–13, 2007.
[34] X. Zong, K. Kim, D. Fang, S. Ran, B. S. Hsiao, B. Chu, *Polymer* **2002**, *43*, 4403.
[35] S. Agrawal, A. Awadhia, *Bull. Mater. Sci.* **2004**, *27*, 523.
[36] J. Gong, L. Luo, S.-H. Yu, H. Qian, L. Fei, *J. Mater. Chem.* **2006**, *16*, 101.
[37] H. S. Mansur, R. L. Oréfice, A. A. P. Mansur, *Polymer* **2004**, *45*, 7193.
[38] A. S. Asran, S. Hernning, G. H. Michler, *Polymer* **2010**, *51*, 868.
[39] S. İşçi, C. Ünlü, O. Atici, N. Güngör, *Bull. Mater. Sci.* **2006**, *29*, 449.